Uptake of ^{11}C-Choline in Mouse Atherosclerotic Plaques

Iina E.K. Laitinen[1], Pauliina Luoto[1], Kjell Någren[1,2], Päivi M. Marjamäki[1], Johanna M.U. Silvola[1], Sanna Hellberg[1], V. Jukka O. Laine[3], Seppo Ylä-Herttuala[4], Juhani Knuuti[1], and Anne Roivainen[1,5]

[1]Turku PET Centre, University of Turku, Turku, Finland; [2]PET and Cyclotron Unit, Department of Clinical Physiology and Nuclear Medicine, Rigshospitalet, University of Copenhagen, Copenhagen, Denmark; [3]Department of Pathology, Turku University Hospital, Turku, Finland; [4]A.I. Virtanen Institute, University of Kuopio, Kuopio, Finland; and [5]Turku Center for Disease Modeling, University of Turku, Turku, Finland

The purpose of this study was to explore the feasibility of ^{11}C-choline in the assessment of the degree of inflammation in atherosclerotic plaques. **Methods:** Uptake of ^{11}C-choline was studied ex vivo in tissue samples and aortic sections excised from 6 atherosclerotic mice deficient for both low-density lipoprotein receptor and apolipoprotein B48 (LDLR$^{-/-}$ApoB$^{100/100}$) and 5 control mice. The autoradiographs were compared with the immunohistology of the arterial sites. **Results:** The uptake of ^{11}C-choline (percentage of the injected activity per gram of tissue) in the atherosclerotic aortas of the LDLR$^{-/-}$ApoB$^{100/100}$ mice was significantly higher (1.9-fold, $P = 0.0016$) than that in the aortas of the control mice. The autoradiography analysis showed significantly higher uptake of ^{11}C-choline in the plaques than in healthy vessel wall (mean ratio, 2.3 ± 0.6; $P = 0.014$), prominently in inflamed plaques, compared with noninflamed plaque areas. **Conclusion:** We observed a high ^{11}C-choline uptake in the aortic plaques of atherosclerotic mice. Our data suggest that macrophages may be responsible for the uptake of ^{11}C-choline in the plaques.

Key Words: atherosclerosis; autoradiography; biodistribution; cardiology; molecular imaging; ^{11}C-choline

J Nucl Med 2010; 51:798–802
DOI: 10.2967/jnumed.109.071704

Atherosclerotic plaque rupture is a major cause of acute cardiac events and stroke. Conventional anatomic imaging may not provide sufficient information for the risk assessment; therefore, the detection and identification of rupture-prone atherosclerotic plaques remains a great clinical challenge. Inflammation and metabolic activity of the plaque are considered key features in terms of plaque vulnerability. High concentrations of inflammatory cells, mainly macrophages, have been demonstrated to be typical of vulnerable plaques (*1,2*). In addition to inflammation, cell proliferation has also been suggested to play an important role in the progression of atherosclerotic plaques, with monocytes or macrophages being the main proliferative cell type in the intimae of human plaques (*3*). Noninvasive imaging of inflammation, together with the possible detection of proliferative cells within atherosclerotic lesions, may be a useful approach for the purpose of predicting future risk of plaque rupture.

Radiolabeled choline and choline analogs have been used in the imaging of various cancer types (*4*). Choline is a source for cell membrane lipids, and all the nucleated cells have specific choline transport mechanisms, varying in expression and being highest in the proliferative cells. Phosphorylated by choline kinase, choline eventually incorporates into cell membranes. Increased choline transport and choline kinase activity in tumor cells and macrophages have been suggested to result in increased choline uptake in these cells (*5,6*).

A recent study demonstrated ^{18}F-fluorocholine uptake in atherosclerotic lesions in a mouse model, with a positive correlation to macrophage staining (*7*). ^{18}F-fluorocholine and ^{11}C-choline have been shown to visualize the vessel wall alterations in the aorta and carotid arteries in cancer patients (*8,9*). The radioactivity was found mainly in the noncalcified vessel wall areas of elderly prostate cancer patients. Without any histologic evidence, however, the true nature of these vessel wall alterations remains unknown, and therefore, further studies are required to establish the uptake of radiolabeled choline in different types of plaques.

The purpose of this study was to explore the feasibility of ^{11}C-choline in the assessment of the degree of inflammation in atherosclerotic plaques using an atherosclerotic mouse model.

MATERIALS AND METHODS

Animals

At the age of 15 mo, male mice deficient for both low-density lipoprotein receptor and apolipoprotein B48 (LDLR$^{-/-}$ApoB$^{100/100}$) (strain 003000; Jackson Laboratory) were fed for 2 mo with a Western-type diet (TD.88137, Adjusted Calories Diet; Harlan). The normally fed male control mice (C57BL) were 13 ± 2 mo old. The study design was approved by the Laboratory Animal Care and Use Committee of the University of Turku, Finland.

Received Oct. 21, 2009; revision accepted Feb. 2, 2010.
For correspondence or reprints contact: Iina E.K. Laitinen, Turku PET Centre, University of Turku, Kiinamyllynkatu 4-8, FI-20520, Turku, Finland.
E-mail: iina.laitinen@gmail.com

Synthesis of ^{11}C-Choline

^{11}C-Choline was produced through the reaction of *N,N*-dimethyl-2-aminoethanol and ^{11}C-methyl triflate using high-performance liquid chromatography purification and analysis procedures described by Rosen et al. (*10*), with high radiochemical yield (>70%) and radiochemical purity (>99.5%).

Biodistribution and Blood Metabolism of ^{11}C-Choline in Atherosclerotic and Control Mice

Six atherosclerotic LDLR$^{-/-}$ApoB$^{100/100}$ mice (mean weight ± SD, 38 ± 3 g) and 5 C57BL control mice (42 ± 6 g) were intravenously injected with ^{11}C-choline (27 ± 10 MBq) via the tail, and after 10 min, the animals were sacrificed under isoflurane anesthesia. Samples of whole blood and tissues (Table 1) were dissected, weighed, and measured for radioactivity using an automatic γ-counter (1480 Wizard 3″; EG&G Wallac). The data were corrected for background and decay. The radioactivity that had accumulated in the tissues was expressed as a percentage of the injected activity per gram of tissue. The plasma was further analyzed for radiometabolites as described earlier (*11*).

Autoradiographic Analysis of ^{11}C-Choline in Aortic Cryosections

The distribution of ^{11}C-choline to the aortic tissue was studied with digital autoradiography as described before (*12*). Briefly, after 1 h of exposure the imaging plates were scanned (Imaging Plate BAS-TR2025 [Fuji]; Analyzer BAS-5000 [Fuji]), and the images of aortic sections were analyzed for count densities (photostimulating luminescence units [PSL]/mm^2) with an image-analysis program (Tina 2.1; Raytest Isotopenmessgeräte GmbH). Three types of regions of interest (ROIs) were defined according to the histology: plaque (excluding the medium), adventitia (containing the adjacent adipose tissue), and healthy vessel wall (Figs. 1A and 1B). The background count densities were subtracted from the image data. ROIs for all visible plaques were drawn over the areas where the plaque was easily identifiable.

TABLE 1. Ex Vivo Biodistribution of ^{11}C-Choline in Atherosclerotic LDLR$^{-/-}$ApoB$^{100/100}$ and Control C57BL Mice at 10 Minutes After Intravenous Injection

Organ	Atherosclerotic (n = 6)	Control (n = 5)	P
Aorta	4.11 ± 1.13	2.21 ± 0.65	0.0016
Blood	0.72 ± 0.20	0.67 ± 0.38	0.7219
Heart	10.84 ± 3.80	8.61 ± 2.23	0.1109
Kidney	23.41 ± 8.00	32.63 ± 21.26	0.5121
Liver	9.53 ± 4.60	10.82 ± 6.20	0.8595
Lung	14.62 ± 6.01	12.94 ± 2.50	0.1981
Muscle	1.29 ± 0.44	1.80 ± 0.65	0.2226
Pancreas	8.44 ± 2.74	8.56 ± 3.09	0.6524
Small intestine	6.57 ± 2.12	5.91 ± 2.55	0.499
Spleen	4.51 ± 2.45	3.62 ± 2.03	0.4593
Thymus	3.11 ± 0.88	2.79 ± 1.62	0.4527
White adipose tissue	0.36 ± 0.12	0.40 ± 0.26	0.8119

Results are expressed as percentage of injected activity per gram of tissue (mean ± SD).

Histology and Immunohistochemistry

After autoradiography, the 20-μm sections were stained with hematoxylin and eosin and studied for morphology under a light microscope. Consecutive 8-μm sections were immunostained with Mac-3 (clone M3/84; BD Pharmingen) or Ki-67 (clone Mib-1; Dako) for the detection of macrophages and proliferating cells, respectively.

Randomly selected plaque areas (n = 35) were semiquantitatively assessed for the degree of inflammation by estimating the number of nuclei and Mac-3–positive cells in consecutive sections, without knowledge of the corresponding autoradiography results. The ROIs in these plaques were divided into 2 categories: noninflamed, with none or occasional leukocytes in the region, and inflamed, with a high number of nuclei and corresponding Mac-3 staining in the area.

Statistical Methods

All the results are expressed as the mean ± SD. Student t test for nonpaired data and Dunnett test were used to compare the biodistribution of ^{11}C-choline in organs. Univariate correlations were calculated using the Pearson partial-correlation method. Repeated-measures ANOVA with Tukey correction was applied to the autoradiography data. Normality was tested using the Shapiro–Wilkins method. A P value less than 0.05 was considered as statistically significant.

RESULTS

Characterization of Atherosclerotic Plaques

All of the studied LDLR$^{-/-}$ApoB$^{100/100}$ mice had developed extensive atherosclerosis throughout the aorta. The observed plaques in the aortas of the LDLR$^{-/-}$ApoB$^{100/100}$ mice contained cell-rich, inflamed areas and acellular necrotic cores. Occasional calcifications were also found. Mac-3 staining revealed areas in the plaques with a moderate number of macrophages (Fig. 1C). Only a few Ki-67–positive cells were detected in the plaques (Fig. 1D).

Ex Vivo Biodistribution and Blood Metabolism of ^{11}C-Choline

The ^{11}C radioactivity measured at 10 min after the injection of ^{11}C-choline was 1.9-fold higher in the aortas of the LDLR$^{-/-}$ApoB$^{100/100}$ mice than those of the C57BL control mice (n = 6 and 5, respectively, P = 0.0016) (Table 1). In the other measured tissues, no significant differences between the atherosclerotic and the control mice were observed. The ^{11}C radioactivity was highest in kidneys, lung, heart, and liver (Table 1). The aorta-to-blood and aorta-to-muscle ratios of the LDLR$^{-/-}$ApoB$^{100/100}$ mice were 5.5 ± 2.2 and 3.0 ± 0.9, respectively. The biodistribution of ^{11}C-choline in the circulating blood was not affected by the animal weight or strain (P = 0.08).

The high-performance liquid chromatography radiodetector analysis of the mouse plasma samples (n = 6) revealed 15% ± 7% of unchanged ^{11}C-choline at 10 min after injection. The percentages of total radioactivity were

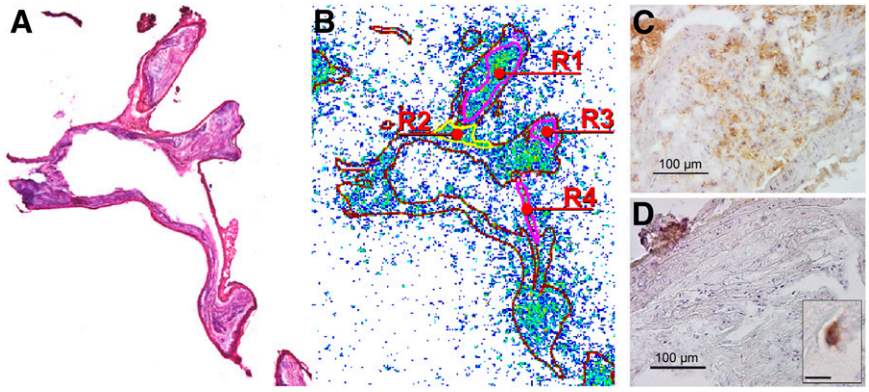

FIGURE 1. Ex vivo autoradiography analysis. (A) Hematoxylin and eosin–stained 20-μm section showing aortic arch and branches. (B) Autoradiography image of same section as in A, with superimposed contour image and delineated ROIs: R1 and R3 = plaque, R2 = adventitia including adjacent adipose tissue, and R4 = wall. (C) Eight-micrometer section showing higher magnification of R1 plaque in brachiocephalic trunk and immunohistochemical staining of macrophages (Mac-3) (bar = 100 μm). (D) Consecutive 8-μm section of same plaque as in C. Immunohistochemical staining with Ki-67 shows few proliferative cells in plaques (bar = 100 μm). Inset shows 1 positive cell at higher magnification (bar = 5 μm).

78% ± 7% for ^{11}C-betaine and 9% ± 3% for another radiometabolite (unidentified).

Autoradiography of Aortic Cryosections

Hematoxylin and eosin–stained longitudinal cryosections throughout the aorta (n = 6–7 sections of each animal) were imaged under a light microscope, and the images were combined with the autoradiographs to define ROIs. The mean uptake of ^{11}C radioactivity in each region was calculated for each mouse (Table 2).

The autoradiography analysis showed a significant uptake of ^{11}C radioactivity in the plaques in comparison to the healthy vessel wall (plaque-to-wall ratio, 2.3 ± 0.6; P = 0.014, n = 6 LDLR$^{-/-}$ApoB$^{100/100}$ mice). The adjacent adventitial tissue, containing the adipose tissue surrounding the vessel, also showed a substantial uptake (adventitia-to-wall ratio, 1.9 ± 0.5; P = 0.016), which, however, was significantly lower than that in the plaques (P = 0.021). No significant uptake was found in calcifications.

The mean plaque-to-wall ratios were 2.6 ± 0.8 and 1.4 ± 0.5 in inflamed and noninflamed plaques, respectively (P < 0.001) (Fig. 2). Most of the cells in the inflamed plaques were identified as macrophages.

TABLE 2. Autoradiography Results of Mean (±SD) ^{11}C-Choline Uptake in ROIs for Each Atherosclerotic Mouse

	Plaque		Adventitia		Wall	
Mouse no.	PSL/mm^2	n	PSL/mm^2	n	PSL/mm^2	n
1	12.3 ± 2.9	29	10.0 ± 2.8	19	4.9 ± 1.5	15
2	10.3 ± 2.0	26	8.7 ± 2.0	18	5.6 ± 1.8	10
3	14.8 ± 4.6	36	12.1 ± 2.4	10	4.5 ± 1.7	14
4	31.7 ± 7.5	25	26.7 ± 8.5	12	15.4 ± 5.0	17
5	12.2 ± 3.5	34	11.5 ± 1.7	6	6.5 ± 1.5	14
6	11.1 ± 3.5	31	8.3 ± 1.8	24	5.7 ± 1.9	19
Mean ratio (to wall)	2.3 ± 0.6		1.9 ± 0.5			
P (vs. wall)	0.014		0.016			

Results are expressed as intensity (PSL/mm^2).

DISCUSSION

Our results revealed a significantly higher uptake of ^{11}C-choline in inflamed atherosclerotic plaques than in healthy vessel wall in LDLR$^{-/-}$ApoB$^{100/100}$ mice. According to autoradiography and ex vivo biodistribution analyses, both the plaque-to-wall ratio and the aorta-to-blood ratio were reasonably high, suggesting the tracer's potential for in vivo PET.

Choline uptake may be amplified either by enhanced transport or by increased choline kinase activity, for example, in cancer cells. In addition to cancer imaging, choline-derived tracers have shown potential for inflammation imaging and accumulation in inflammatory cells (*5,13*). The metabolic activity and the production of nitric oxide may explain the choline uptake in macrophages (*14*), but this requires further study.

Our study showed a 1.9-fold higher uptake of ^{11}C-choline in the aortas of the atherosclerotic mice than in the aortas of the control mice. Our biodistribution results are in accordance with the results of previous studies (*15–17*). At 10 min after injection, the target-to-background (aorta-to-blood) ratio was 5.5, indicating fast blood clearance. We observed high uptake in the heart and kidneys, which could be problematic when imaging these targets. However, there seems to be a species difference, because low myocardial uptake has been previously reported in humans (*7,9*). Choline and its metabolites such as betaine or acetylcholine may have a different cardiac uptake pattern in rodents.

The autoradiography analysis revealed 2.3-fold higher uptake in plaques in general and 2.6-fold higher uptake in the inflamed plaques than the healthy vessel wall. In noninflamed plaques, the plaque–to–normal wall ratio was significantly lower, suggesting that inflammatory cells, mainly macrophages, may be the reason for increased

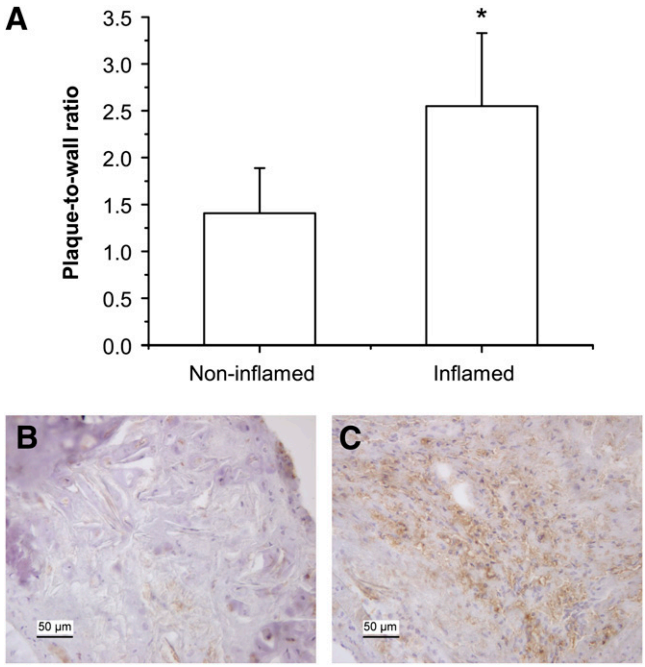

FIGURE 2. (A) Uptake of ^{11}C-choline in mouse atherosclerotic plaques ($n = 20$ [noninflamed] and 15 [inflamed], $^*P < 0.001$). Plaque-to-wall ratio was calculated for each plaque region against mean PSL/mm^2 value of healthy wall uptake of same animal. (B) Immunohistochemical Mac-3 staining of noninflamed plaque area, showing only occasional macrophages. (C) Mac-3 staining of inflamed plaque, showing high number of macrophages. Bar = 50 μm.

uptake. Relatively high uptake in adventitia requires further study but is likely due to resident macrophages and possibly to infiltrated leukocytes.

Previously, for ^{18}F-fluorocholine, a plaque–to–normal wall ratio of nearly 5 was reported in ApoE$^{-/-}$ mice (*7*) (achieved using an en face autoradiography method). Microautoradiography of the aortic sections, which is comparable to the method used in this study, revealed a plaque-to-wall ratio of 3.5. However, ^{11}C-choline and ^{18}F-fluorocholine are 2 different compounds with divergent pharmacokinetic properties; thus, no direct comparison can be made.

Choline uptake has been previously shown to correlate with proliferative activity in the tissue (*6*). However, the overall proliferative activity in the plaques was low, only 0.49% (*18*). In our study, only a few Ki-67–positive cells were found in the plaques, and this cannot explain the found uptake.

Although we found a significant difference between the biodistribution of ^{11}C-choline to the atherosclerotic and the healthy aortas, we used only a limited number of animals in this study. However, the autoradiography analysis was performed in multiple sections covering all the plaques to better estimate the distribution to different plaques. The analysis also showed that the uptake varied depending on the plaque morphology.

CONCLUSION

We observed that ^{11}C-choline uptake in the atherosclerotic plaques was significantly increased as compared with the healthy vessel wall. Our findings suggest that macrophages may be responsible for the higher uptake of ^{11}C-choline in the plaques. Although uptake of ^{11}C-choline was prominent in the atherosclerotic plaques in this animal model, further clinical studies are needed to elucidate the value of ^{11}C-choline as a marker of plaque inflammation for in vivo imaging.

ACKNOWLEDGMENTS

We thank Erica Nyman for technical assistance and Irina Lisinen for statistical analysis. This work was funded by the Instrumentarium Foundation, Finnish Cultural Foundation, Turku University Foundation, Academy of Finland (no. 119048), Hospital District of Southwest Finland, and Drug Discovery Graduate School. The study was conducted within the Finnish Centre of Excellence in Molecular Imaging in Cardiovascular and Metabolic Research, which is supported by the Academy of Finland, University of Turku, Turku University Hospital, and Åbo Akademi University.

REFERENCES

1. Moreno PR, Bernardi VH, Lopez-Cuellar J, et al. Macrophages, smooth muscle cells, and tissue factor in unstable angina: implications for cell-mediated thrombogenicity in acute coronary syndromes. *Circulation.* 1996;94:3090–3097.
2. Naghavi M, Libby P, Falk E, et al. From vulnerable plaque to vulnerable patient: a call for new definitions and risk assessment strategies—part I. *Circulation.* 2003;108:1664–1672.
3. Rekhter MD, Gordon D. Active proliferation of different cell types, including lymphocytes, in human atherosclerotic plaques. *Am J Pathol.* 1995;147:668–677.
4. Tian M, Zhang H, Oriuchi N, et al. Comparison of ^{11}C-choline PET and FDG PET for the differential diagnosis of malignant tumors. *Eur J Nucl Med Mol Imaging.* 2004;31:1064–1072.
5. Wyss MT, Weber B, Honer M, et al. ^{18}F-choline in experimental soft tissue infection assessed with autoradiography and high-resolution PET. *Eur J Nucl Med Mol Imaging.* 2004;31:312–316.
6. Yoshimoto M, Waki A, Obata A, et al. Radiolabeled choline as a proliferation marker: comparison with radiolabeled acetate. *Nucl Med Biol.* 2004;31:859–865.
7. Matter CM, Wyss MT, Meier P, et al. ^{18}F-choline images murine atherosclerotic plaques ex vivo. *Arterioscler Thromb Vasc Biol.* 2006;26:584–589.
8. Bucerius J, Schmaljohann J, Bohm I, et al. Feasibility of ^{18}F-fluoromethylcholine PET/CT for imaging of vessel wall alterations in humans: first results. *Eur J Nucl Med Mol Imaging.* 2008;35:815–820.
9. Kato K, Schober O, Ikeda M, et al. Evaluation and comparison of ^{11}C-choline uptake and calcification in aortic and common carotid arterial walls with combined PET/CT. *Eur J Nucl Med Mol Imaging.* 2009;36:1622–1628.
10. Rosen MA, Jones RM, Yano Y, et al. Carbon-11 choline: synthesis, purification, and brain uptake inhibition by 2-dimethylaminoethanol. *J Nucl Med.* 1985;26:1424–1428.
11. Roivainen A, Forsback S, Grönroos T, et al. Blood metabolism of [methyl-^{11}C]choline; implications for in vivo imaging with positron emission tomography. *Eur J Nucl Med.* 2000;27:25–32.
12. Laitinen I, Marjamäki P, Någren K, et al. Uptake of inflammatory cell marker [^{11}C]PK11195 into mouse atherosclerotic plaques. *Eur J Nucl Med Mol Imaging.* 2009;36:73–80.
13. Roivainen A, Parkkola R, Yli-Kerttula T, et al. Use of positron emission tomography with methyl-^{11}C-choline and 2-^{18}F-fluoro-2-deoxy-D-glucose in

comparison with magnetic resonance imaging for the assessment of inflammatory proliferation of synovium. *Arthritis Rheum.* 2003;48:3077–3084.
14. Sands WA, Clark JS, Liew FY. The role of a phosphatidylcholine-specific phospholipase C in the production of diacylglycerol for nitric oxide synthesis in macrophages activated by IFN-γ and LPS. *Biochem Biophys Res Commun.* 1994; 199:461–466.
15. Zheng QH, Stone KL, Mock BH, et al. [^{11}C]Choline as a potential PET marker for imaging of breast cancer athymic mice. *Nucl Med Biol.* 2002;29:803–807.
16. Zheng QH, Gardner TA, Raikwar S, et al. [^{11}C]Choline as a PET biomarker for assessment of prostate cancer tumor models. *Bioorg Med Chem.* 2004;12:2887–2893.
17. Henriksen G, Herz M, Hauser A, et al. Synthesis and preclinical evaluation of the choline transport tracer deshydroxy-[^{18}F]fluorocholine ([^{18}F]dOC). *Nucl Med Biol.* 2004;31:851–858.
18. Brandl R, Richter T, Haug K, et al. Topographic analysis of proliferative activity in carotid endarterectomy specimens by immunocytochemical detection of the cell cycle-related antigen Ki-67. *Circulation.* 1997;96:3360–3368.

The Journal of NUCLEAR MEDICINE

Uptake of ^{11}C-Choline in Mouse Atherosclerotic Plaques

Iina E.K. Laitinen, Pauliina Luoto, Kjell Någren, Päivi M. Marjamäki, Johanna M.U. Silvola, Sanna Hellberg, V. Jukka O. Laine, Seppo Ylä-Herttuala, Juhani Knuuti and Anne Roivainen

J Nucl Med. 2010;51:798-802.
Published online: April 15, 2010.
Doi: 10.2967/jnumed.109.071704

The Journal of Nuclear Medicine is published monthly.
SNMMI | Society of Nuclear Medicine and Molecular Imaging
1850 Samuel Morse Drive, Reston, VA 20190.
(Print ISSN: 0161-5505, Online ISSN: 2159-662X)

SNMMI SOCIETY OF NUCLEAR MEDICINE AND MOLECULAR IMAGING